ACCELERATED PARAMETERIZED COMPUTATION OF THE THERMAL BEHAVIOUR OF DUAL PURPOSE CASKS

Roppel, Matthias (1);
Lange, Christopher (1);
Roith, Bernd (2);
Rieg, Frank (1)

1: University of Bayreuth;
2: Swiss Federal Nuclear Safety Inspectorate ENSI

ABSTRACT

One of the fundamental requirements for dual purpose casks, which are used for the transport and interim storage of spent fuel assemblies, is the safe removal of the resulting decay heat. To ensure this the temperature fields are determined using numerical methods. However, their modelling is complex and the computation time-consuming.
In order to accelerate this thermal assessment, we have developed z88ENSI, an independent simulation tool based on finite element analysis. With regard to the modelling, various parameters can be varied quickly with our newly designed mesh manipulation procedure. Concerning the computation time, we developed and implemented an approach for calculating three-dimensional temperature fields, based on an already existing two-dimensional method which lacked precision. We accelerate the calculation by using extended thermal gap constraints, which depict the thermal behaviour of the non-meshed, gas-filled gaps inside the cask. We validate the results of our calculation tool by comparing them with those generated with Ansys. The results of the comparison temperatures differ between -0.8% and 3.7%. The speedup of z88ENSI for the specific validation setting is between 6.9 and 15.0.

Keywords: Numerical methods, Product modelling / models, Simulation

Contact:
Roppel, Matthias Oliver
University of Bayreuth
Chair of Engineering Design and CAD
Germany
matthias.roppel@uni-bayreuth.de

Cite this article: Roppel, M., Lange, C., Roith, B., Rieg, F. (2021) 'Accelerated Parameterized Computation of the Thermal Behaviour of Dual Purpose Casks', in *Proceedings of the International Conference on Engineering Design (ICED21),* Gothenburg, Sweden, 16-20 August 2021. DOI:10.1017/pds.2021.32

1 INTRODUCTION

After their time in containment spent fuel assemblies are transported and stored in so called dual-purpose casks (DPC). In order to meet the safety requirements, among other things, the temperature fields inside the loaded DPC must be precisely determined, especially at certain critical points. Due to the complexity of the casks and the thermal processes, numerical methods are used for this determination. However, performing numerical simulations is very time-consuming, because detailed models usually have several million degree of freedoms, resulting from their complex geometry and the need for high resolution. In addition, each cask has an individual load with spent fuel assemblies and thus its own thermal profile. Therefore, a large number of thermal simulations are necessary both in the design processes and in approval procedures of DPC. Concerning the approval procedures of the thermal calculations, two factors need to be evaluated by the supervisory authorities, who are entrusted with the approval of casks, their loading with spent fuel assemblies, their transport and interim storage: First, they have to check the thermal calculations of the applicant and the maximum allowable temperatures at the critical points. Second, they have to evaluate the basic assumptions and simplifications for those calculations. Due to the high variance of different cask types, loadings, configurations and thermal models, the evaluation by re-modelling with general-purpose software is very time-consuming. In order to optimize the workflow, it is advisable to automate and accelerate these thermal simulations as far as possible.

In this contribution, we present a further developed independent simulation tool for determination of a DPC's temperature field, based on finite-elements. It enables a fast, approximate but sufficiently accurate determination of the temperature field inside of various DPC for spent fuel assemblies. Basis of the simulation tool is the quasi two-dimensional method presented by Dinkel (2019). Furthermore, various parameters can be varied easily by a newly implemented mesh manipulation procedure in order to determine their effects on the temperature field. We validate our tool by comparing the results with those of simulations with the commercial software Ansys.

Before we present and verify our approach and describe our mesh manipulation procedure, a brief description of the function and basic structure of the DPC follows. In addition, the basic effect of high temperatures to the structure of the casks and the resulting need to limit the temperatures at various critical points are explained.

2 DUAL PURPOSE CASKS

In all common light water reactor concepts fuel assemblies are removed from the reactor at the end of their working time and transferred to the fuel pool. There, the resulting decay heat is dissipated by active cooling over a certain period of time. If it falls below a certain threshold, the spent fuel assemblies can be stored dry. For this purpose, DPC are used (Fentiman, 2018). DPC must guarantee four different protection goals over their entire service lifetime. In addition to prevent damage caused by heat, these include the containment of the radioactive contents, the control of the external dose rate and the prevention of criticality (IAEA, 2018). In addition to these requirements, an idea of the general structure of DPC is important for the following explanations. In simplified terms, a DPC consists of a basket, a cask body, a primary lid and a secondary lid, as shown in Figure 1.

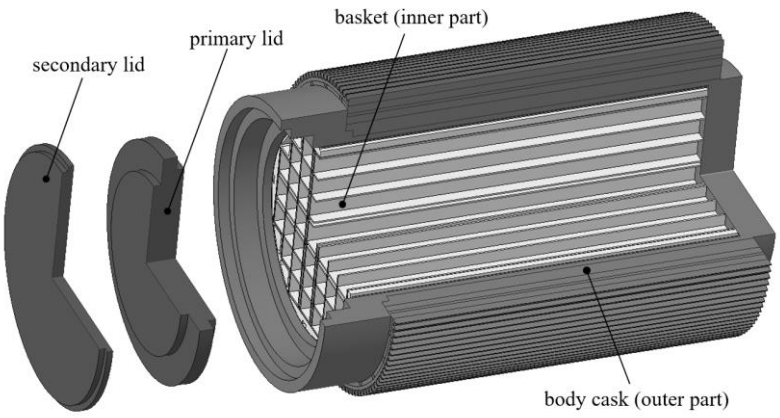

Figure 1. Simplified structure of a DPC

https://doi.org/10.1017/pds.2021.32 Published online by Cambridge University Press

The grid-like structured basket stores the spent fuel assemblies. The cask's outer part has a high mechanical durability and shields ionizing radiation. A dual lid system guarantees the secure closure of the spent fuel assemblies (Droste et al., 2014). Inside the cask, there are gaps even in the closed state due to manufacturing, assembly and use. They can for example be found between the basket and the cask body. These cavities are filled with gas such as helium or nitrogen. These gases have comparatively good thermal conductivity properties, in order to achieve the best possible heat dissipation. To monitor the tightness of the system, a negative pressure is applied between the two lids. For this reason, there are gaskets between the respective lid and the cask body. DPCs usually have an overall diameter between two to three meters, while being approximately six meters high. A fully loaded cask weighs around 100 tons (Fentiman, 2018). These are exemplary values.
As already mentioned, the safe removal of the decay heat is one of the four protection goals of a DPC. Namely if the generated head exceeds a certain threshold, it endangers the integrity of the fuel assembly structure and further that of the cask. This is due to the temperature dependence of the material parameters, e.g. the yield strength, tensile strength and modulus of elasticity decrease with increasing temperature. At the same time, especially metallic materials expand with increasing temperatures. Temperature differences lead to different degrees of expansion and furthermore, individual parts in assemblies cannot expand freely in all directions. This results in thermal stresses. These thermal stresses superpose the mechanical stresses and the overall load increases (Petersen, 1983), (Meetham and Van de Voorde, 2000). Hence, cask specific maximum temperatures are defined for DPC at various critical points. As an example, for the HI-STAR 180 cask designed by Holtec International the following maximum temperatures are defined: cask surface 391 K, secondary lid gasket 374 K, primary lid gasket 387 K, basket 548 K and fuel rod cladding tube 578 K (Holtec International, no date).

3 CONSIDERATION OF AXIAL HEAT FLOWS WITH DIFFERENT GAP WIDTHS IN THE THERMAL SIMULATION OF DUAL PURPOSE CASKS

3.1 Fundamental problem and approach

The main requirement for our software tool is the fast computation of the results with sufficient accuracy. In general, the calculation time highly correlates with the structure, the physical state of the materials and the considered heat transfer mechanisms. With regard to the structure of DPC, the following can be stated: On the one hand, there are large, massive solid bodies, such as the basket, the lids or the cask body; on the other hand, there are many narrow but long gas filled gaps. The effect of the gaps is insulation in terms of heat dissipation, which is based on the lower thermal conductivity of the gas in contrast to the surrounding metallic components. Therefore, those gaps have to be considered when determining temperature fields. A fine discretization is necessary for numerical simulation, in order to map the thermal behaviour of the gaps correct. But the finer the mesh, the longer the computation time. Concerning the physical state of the materials, heat dissipation of DPC is a multiphasic problem. Furthermore, all three heat transfer mechanism occur. DPC has both solid and fluid areas. In solids heat conduction occurs as the only heat transfer mechanism. When heat transfers from a solid to a fluid, convection mechanisms have to be considered. In order to simulate the convective heat transfer, flow simulations are necessary. In addition to conduction and convection, radiation transfers heat across the gap. Thermal radiation itself is a non-linear process that is calculated numerically iteratively. Moreover, the mutual visibility of the surfaces involved in the exchange of radiation is important. With regard to numerical modeling and calculation, for example with the Finite Eelement Method (FEM), convection and radiation are considerably more complex than with pure heat conduction and increase the computation time (Marek et al. 2019) (Reddy et al. 2010).
In order to enable rapid thermal simulations of DPC, but still deliver sufficiently accurate results, we have been following a FEA-only approach, in which only the solid components are considered. The fuel assemblies are not taken into account as physical components, only their decay heat placed on the shaft walls of the basket is given as a boundary condition. The gas-filled gaps are not meshed, so the nodes of the inner and outer cask parts are not connected with finite elements, see Figure 3. In principle, heat transfer between an inner and an outer gap note corresponds to an additional constrain that must be integrated into the overall system of equations. This problem is analogous to mechanical contact problems, in which even unconnected nodes must be related to each another. Various mathematical methods exist for this purpose, such as the penalty method or

https://doi.org/10.1017/pds.2021.32 Published online by Cambridge University Press

the Lagrange multipliers method (Cook et al. 2002). Both methods have different advantages and disadvantages. We do not present them in this paper and refer to Wriggers (2006). Combinations of both methods, such as the perturbed Lagrange multiplier method, eliminate the individual disadvantages of each method and the strengths come into their own. However, they cause an overall increase of the computational effort (Rust 2016).
Dinkel (2019) combines the perturbed Lagrange multiplier method with analytical equations that depict heat transfer by conduction, convection and / or thermal radiation and refers to this approach as thermal gap conditions (TGC). The use of TGC achieves significant advantages like a decreased modelling effort and reduced computing time.

3.2 Initial situation and extension

Dinkel's (2019) existing formulation and implementation of TGC was just for two-dimensional problems, in which only the middle part of DPC at the height of the basket was considered. In other words, the investigated system has neglected the axial head fluxes to the lids and the bottom. Thus only the radial dissipation of the decay heat was considerable. Furthermore, there were only two possible positions of the basket inside the cask body: the storage and transport position, see Figure 3 (Dinkel et al., 2019).
The purely radial heat dissipation is basically a conservative approach, but the verifiability and significance are considerably restricted. For this reason, our focus has been on the integration of the axial heat flows, because these lead to significant changes in the temperature field. This becomes clear in the following example, simulated with Ansys: The minimal model also used later for verification is considered. For the three-dimensional calculation the minimal model in the initial position is used. For the quasi-two-dimensional calculation the same model is used, but the top and bottom are cut off and the cut surfaces are considered to be adiabatic. Figure 2 shows both models in cut views. All other simulation settings and boundary conditions are analogous to the verification, we describe in section 3.5. With the quasi two-dimensional view, the entire heat is dissipated radially and the result is a maximum temperature of 462 K. With the three-dimensional view, the heat is only dissipated to 80 % radially and to 10 % towards the top or bottom. The maximum temperature is 393 K, which is 15 % lower. This example makes it clear that reliable results for DPC can only be obtained with more realistic three-dimensional models. Therefore, we extend the TGC. This extension makes a completely new implementation necessary, which we realize in the current version of our simulation tool z88ENSI.

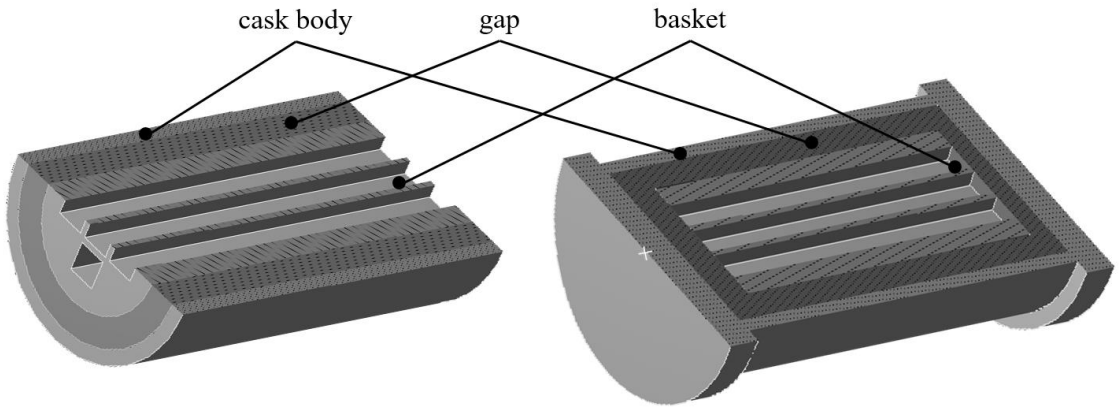

Figure 2. Quasi two-dimensional (left) and three-dimensional (right) minimal model of DPC

In principle, our approach is applicable to other applications, but three important requirements must be met. The fluid must be in a closed space surrounded by solid components. Furthermore, there must be analytical equations that describe the thermal behaviour of the fluid, and the mesh in the gap area must conform.
As already mentioned at the beginning, the three-dimensional calculation of temperature fields and the need to vary all gap dimensions within certain limits lead to a new mesh manipulation procedure. We describe this in the following, also because it is important for understanding the TGC extension.

https://doi.org/10.1017/pds.2021.32 Published online by Cambridge University Press

3.3 Cask positions and gap shapes

With the further developed three-dimensional approach, there are three gap areas depending on the position of the inner cask part and its dimensions: the radial gap between basket and cask body, the upper axial gap between basket and primary lid and the lower axial gap between basket and the bottom of the cask body. Due to the manufacturing and assembly conditions, the dimensions of the components have certain tolerances, which means that the width of the gaps can vary. The position of the inner cask part on the outer one determines the shape of the gaps. In addition to the two positions (storage, transport) that already exist in the two-dimensional case, we have identified two further positions (initial, handling) that are important for the thermal evaluation of DPC. All four positions, which are also shown in Figure 3, are listed below:

- The initial position, in which the inner cask part hovers within the outer one. This position, which does not occur in reality, is only interesting for the thermal evaluations due to its conservative character. The gaps act like a thermal barrier in every direction, leading to little heat dissipation. The shapes of the gaps, which are important for the TGC, are flat and horizontal for the axial and circular for the radial direction.
- The storage position represents the positioning of the inner and outer container during a DPC's intermediate storage. The inner cask is concentric within the outer one. The radial gap is again circular, the upper axial one is flat and horizontal and the lower one does not exist, so a thermal contact is established in this area.
- In the handling position, which may occur during transfer or lifting processes, the inner container has both thermal surface and line contact with the outer container part. The radial gap is sickle-shaped, the upper axial one is flat and inclined, and the lower one does not exist.
  In the transport position, the inner cask part is lying within the outer cask body. This is the most unfavourable position of the cask parts due to the long-term thermal contact when trucks or trains transport the DPCs in a horizontal position. The radial gap is sickle-shaped; the upper axial one is flat and vertical, just like the lower one.

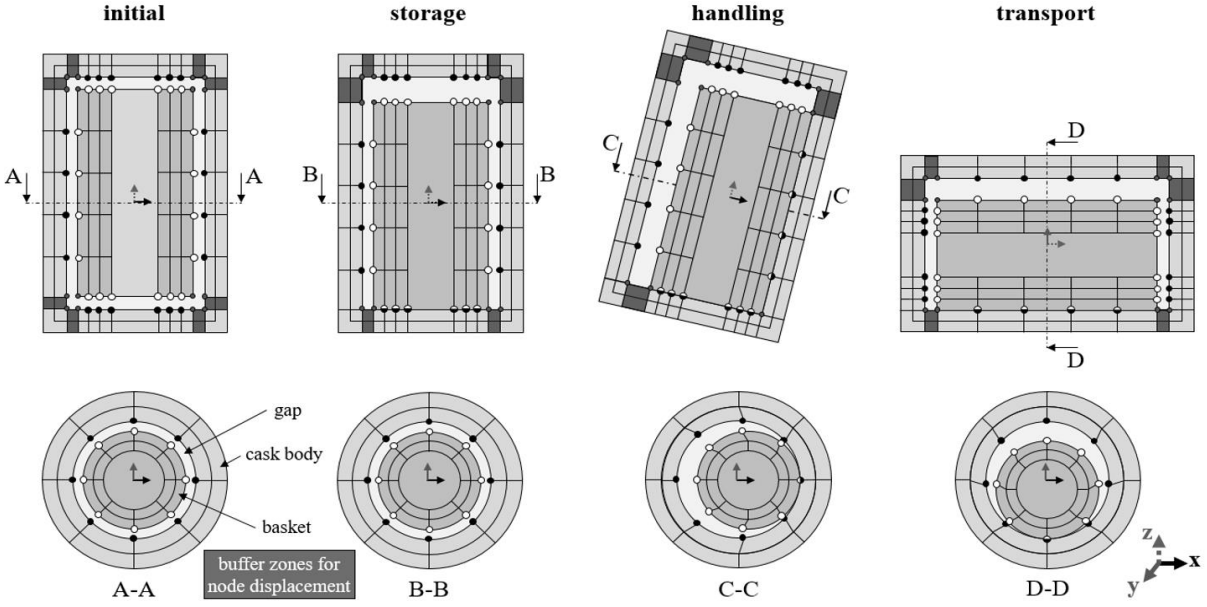

Figure 3. Possible positions of the cask components and visualization of the gap variation

Besides different positions of outer and inner cask, the tolerance of the gaps has to be considered as well. Prior entering the solver, the simulation tool conducts a mesh manipulation in order to enable the assessment of various combinations of positions and gap widths. Regardless of the cask type, the procedure is as follows: Starting with the initial position a mesh manipulation module adjusts the mesh in order to achieve the desired gap widths for the radial and both axial gaps. First, the module varies the radial gap. Next, the module conducts a node displacement of the inner cask to achieve the desired axial position. Since the formulation of the TGCs require node-to-node-coupling, nodes of both, the inner and outer casks, are aligned by changing the size of so-called buffer zones (indicated with dark-grey in the upper part of Figure 3). However, in the case of the handling or transport position, this would lead to an ambiguous mapping of nodes, which could lead to a wrong computation of the

https://doi.org/10.1017/pds.2021.32 Published online by Cambridge University Press

temperature field. Therefore, a node correction procedure adjusts the alignment of nodes (indicated in the sectional views of handling and transport position in Figure 3). Last, the mesh manipulation module varies the axial gaps. Again, changing the size of the buffer zones ensures a node-to-node-coupling.
To provide extendibility of our procedure, we have defined the following specifications that all cask models have to fulfil:

- The initial position is the starting model and has always maximum gap dimensions.
- The dimensions of the outer cask are not manipulated.
- In the gap areas a structured mesh is required, so that the one node of the inner cask and one node of the outer cask form a gap node pair.
- The distance between a gap node pair has to be minimal. Therefore, the nodes are reframed.

3.4 Enhanced formulation of thermal gap conditions for axial gaps

In this section, we are describing the enhanced formulation of TGC, which now includes axial gaps. As already mentioned, the gap between inner and outer cask is not meshed but coupled by means of analytical equations, allowing a fast and sufficient determination of the temperature field.
By the use of the TGC, the analytical equations that depict heat transfer by conduction, convection and/ or thermal radiation are inserted into the overall system of equations of the FEA model by using the perturbed Lagrange multiplier method as described in formula (1).

$$\boldsymbol{KT} = \begin{bmatrix} \boldsymbol{K_{c1}} & 0 & 1 \\ 0 & \boldsymbol{K_{c1}} & -1 \\ 1 & -1 & \alpha_{dL}^{-1} \end{bmatrix} \begin{pmatrix} \boldsymbol{T_{c1}} \\ \boldsymbol{T_{c2}} \\ \boldsymbol{\lambda_{dL}} \end{pmatrix} = \begin{pmatrix} \boldsymbol{Q_{c1}} \\ \boldsymbol{Q_{c2}} \\ \boldsymbol{W} \end{pmatrix} = \boldsymbol{Q} \tag{1}$$

After the thermal conductivity matrices of the two cask parts $\boldsymbol{K_{c1}}$ and $\boldsymbol{K_{c2}}$ have been generated and assembled to the total thermal conductivity matrix $\boldsymbol{K}$, boundary conditions are integrated. Multi-point-constraints connect the gap nodes pairs. For integration, these are formulated as

$$T_i - T_o = W \tag{2}$$

with T_i as node temperature of the inner node and T_o for the corresponding node on the outer cask. W is a heat transfer function. To implement a coupling, a row and a column are added to the total thermal conductivity matrix containing only zero values except the diagonal matrix element and the affected degree of freedom, see equation (1). The non-zero entities can either have -1 or +1 value, indicating the direction of the heat flow. In order to avoid numerical instability of the matrix, a penalty term α_{dL}^{-1} is written on the corresponding diagonal matrix entities. The temperature vector $\boldsymbol{T}$ and heat vector $\boldsymbol{Q}$ are supplemented as well for each gap node pair. For T the Lagrange multiplier $\boldsymbol{\lambda_{dL}}$, which is an additional unknown, is added and the heat transfer function W is entered in vector $\boldsymbol{Q}$. These transfer functions correspond to the analytical equations that represent the heat transfer behaviour of the respective gap nodes (Dinkel, 2019).
VDI (2010) and Marek et al. (2019) contain the analytical equations presented in the following. The basic equation for considering various heat transfer mechanisms is the analytical equation for pure heat conduction through a flat layer

$$T_i - T_o = W = \frac{Q\, s_{gap}}{A\, \lambda_{var}} \tag{3}$$

with Q as the heat flow through the gap, s_{gap} as gap width and A is flown through area. The individual heat transfer mechanisms or respectively their combinations are taken into account by using the placeholder λ_{var}. This variable can represent thermal conductivities for the superposition of various heat transfer mechanisms:

$$\lambda_{var} = \lambda_c \vee \lambda_{cc} \vee \lambda_r \vee \lambda_{ccr} \vee \lambda_{cr} \vee \lambda_{con} \tag{4}$$

$$\lambda_c = \lambda_{fluid} \tag{5}$$

$$\lambda_{cc} = \lambda_c\, Nu \tag{6}$$

https://doi.org/10.1017/pds.2021.32 Published online by Cambridge University Press

$$\lambda_r = 4\sigma_{io} s_{gap} T_m^3 \tag{7}$$

$$\lambda_{cr} = \lambda_c + \lambda_r \tag{8}$$

$$\lambda_{ccr} = \lambda_{cc} + \lambda_r \tag{9}$$

$$\lambda_{con} = \text{constant} \tag{10}$$

Here, λ_c corresponds to the thermal conductivity with pure thermal conduction and only the material value of the gas λ_{fluid} is used. Convection is mapped with λ_{cc} by manipulating the thermal conductivity of the fluid with the Nusselt number Nu. The Nusselt number is calculated according to different relationship, depending on the shape and orientation of the gap. Pure radiation is considered by λ_r or in combination with conduction by λ_{cr} or in combination with conduction and convection by λ_{ccr}. The calculation of radiation includes the radiation constant of the arrangement σ_{io} includes the emissivity of the materials that are important for radiation as well as the geometric conditions. T_m corresponds to the mean temperature in the gap and s_{gap} to the respective gap width. Depending on the position, different surfaces of the inner and outer cask are in contact with each other, heat conduction is also required for the thermal contact case by λ_{con}. In order to achieve an ideal thermal contact, this thermal conductivity has a correspondingly high value.

The basic equations for considering all heat transfers occurring in DPC are thus shown. The gap-dependent equations for determining the Nusselt number and the radiation parameters follow.

With convection, there are different gap orientations, which occur depending on the cask position. The Nusselt number in a flat horizontal gap can be calculated with

$$Nu = 1 + 1{,}44\ max\left[\left(1 - \frac{1708}{Ra}\right), 0\right] + max\left[\left(\frac{Ra^{\frac{1}{3}}}{18} - 1\right), 0\right] \tag{11}$$

Here, Ra is the Rayleigh number. This formula applies to the upper and lower gap of the initial position and to the upper gap of the storage position. Formula (12) describes the determination of the Nusselt number for the flat and inclined gap in handling position

$$Nu = 1 + 1{,}44\ max\left[\left(1 - \frac{1708}{Ra}\right), 0\right]\left(1 - \frac{1708\,[sin(1{,}8\,\gamma)]^{1{,}6}}{Ra\cos\gamma}\right) + max\left[\left(\frac{(Ra\cos\gamma)^{\frac{1}{3}}}{18} - 1\right), 0\right] \tag{12}$$

whereby a value of 45° is chosen for the angle of inclination γ.

For the axial gaps of horizontal DPC (e.g. in transport position,) the following relationship applies to the determination of the convective heat transfer in the flat, vertical gaps:

$$Nu = \left[1 + \left(\frac{0{,}0665\ Ra^{\frac{1}{3}}}{1 + \left(\frac{9000}{Ra}\right)^{1{,}4}}\right)^2\right]^{0{,}5} \tag{13}$$

After considering the convective calculation rules, the formulas used for thermal radiation are presented. The formula for the constant of the arrangement σ_{io} is

$$\sigma_{io} = \frac{\sigma}{\frac{1-\varepsilon_i}{\varepsilon_i} + \frac{1}{F_{io}} + \frac{1-\varepsilon_o}{\varepsilon_o}\frac{A_i}{A_o}} \tag{14}$$

The index i indicates the emissivity and the area of the inner cask's surface and the index o for the outer cask. The Stefan-Boltzmann constant σ is also included in the calculation, as the view factor F_{io}

https://doi.org/10.1017/pds.2021.32 Published online by Cambridge University Press

between the two surfaces involved in the radiation exchange. Formula (15) for two parallel disks of the same size approximates the view factor for the axial gaps, with R as the radius of the disks.

$$F_{\mathrm{io}} = \frac{s_{gap}^2}{2\,R^2}\left(1 + \frac{2\,R^2}{s_{gap}^2} - \sqrt{1 + \frac{4\,R^2}{s_{gap}^2}}\right) \tag{15}$$

Based on these analytical formulas for the axial gaps in combination with the TGC and the corresponding formulas for radial gaps according to Dinkel (2019), the three-dimensional dissipation of the decay heat in DPC can be determined depending on the heat transfer mechanisms.
We have implemented this mesh manipulation procedure and the further developed TGC in the simulation tool z88ENSI. The next section shows the Verification with commercial software

3.5 Verification of the approach

We verified the extended TGC by modelling a DCP with the commercial FEA software Ansys and the conventional approach by meshing the gaps.
The subject of comparison is a minimal model in the storage position and conduction transfer the heat in the gaps. The inner cask has an outer diameter of 50 mm and a height of 100 mm before mesh manipulation. Arranged symmetrically around the center, there are five shafts with a square cross-section with a side length of 10 mm and a distance of 2 mm from one another. They extend completely over the entire height of the inner cask. The outer cask is a hollow cylinder with an inner diameter of 70 mm and an inner height of 120 mm. The wall thickness of the cylindrical part is 5 mm, that of the top and bottom 10 mm. At the level of the lid and the bottom, the outer cask has collars with an outer diameter of 90 mm and a height of 10 mm each. Figure 4 shows the structure of the minimal model.

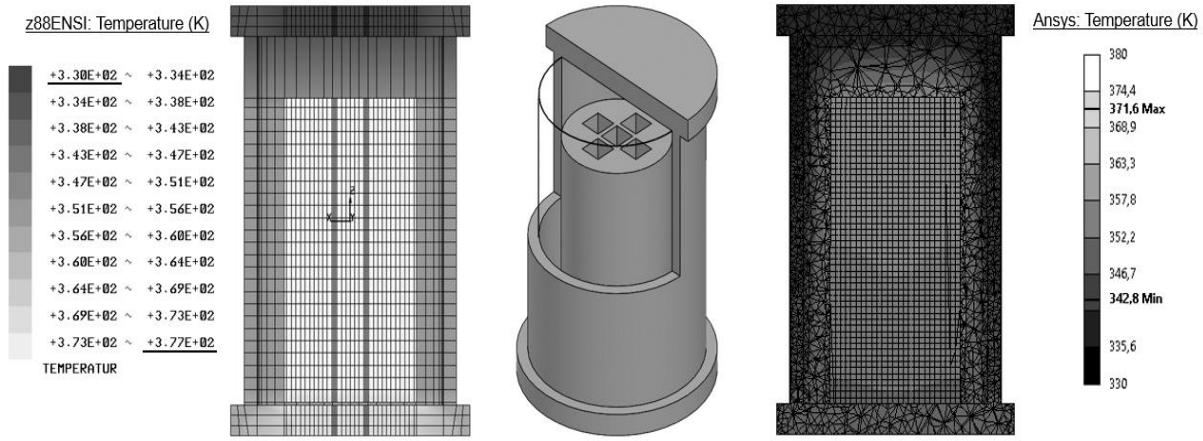

Figure 4. Minimal model with an axial gap of 20mm and a radial gap of 10mm (centre), simulation results of these gap dimensions with z88ENSI (left) and the comparison software ansys (right)

We choose the following thermal boundary conditions and material parameters: A total heat flow of 25 W is applied to all shaft walls of the five fuel assembly shafts. There is a convective boundary condition on all outer surfaces of the outer cask, with the exception of the floor surface. This surface is adiabatic. The heat transfer coefficient is 10 W/m^2K and the ambient temperature is 293.15 K. The thermal conductivity of both cask parts is 60.5 W/mK. The thermal conductivity for the fluid is 0.195 W/mK. The thermal contact has a thermal conductivity of 9000 W/mK.
The comparative calculations are made using the steady-state thermal module of Ansys Workbench 19.2. The gap is meshed with tetrahedron and hexahedron with a program-controlled element order. The element size is 2 mm. The gap elements have the thermal conductivity of the fluid.
Amongst others, three temperatures are important for the design and assessment of DPCs:

- The maximum container temperature T_{max}.
- The maximum gasket temperature on the inner, upper edge of the outer casks $T_{max,g}$.
- The maximum temperature on the outer surface of the outer container $T_{max,s}$.

The axial gaps are varied between 20 mm and 1 mm and the radial one between 10 mm and 1 mm.

https://doi.org/10.1017/pds.2021.32 Published online by Cambridge University Press

Figure 4 compares exemplary two results of z88ENSI (left) and Ansys (right). Table 1 shows the simulation results of z88ENSI for different gap size combinations and the relative deviations to the Ansys results. The CPU times of both tools are also given.

Table 1. Comparison of calculated total maximum temperature T_{max}, maximum gasket temperature $T_{ma}T_{max,gx,g}$ and maximum surface temperature $T_{max,s}$ and the CPU times

gap		T_{max}		$T_{max,g}$		$T_{max,s}$		$CPU\ time$	
axial	radial	z88ENSI	deviation to Ansys	z88ENSI	deviation to Ansys	z88ENSI	deviation to Ansys	z88ENSI	Ansys
(mm)	(mm)	(K)	(%)	(K)	(%)	(K)	(%)	(s)	(s)
20	10	377.4	0.2	337.3	3.7	371.7	-0.8	7.3	55.2
20	7	372.2	0.5	339.3	3.2	366.2	0.3	7.4	57.9
20	4	366.9	0.6	338.8	3.5	362.5	0.7	7.4	76.6
20	1	358.8	0.9	341.1	3.2	356.4	1.1	7.3	110.1
14	10	375.1	0.7	341.2	2.6	369.5	-0.4	7.4	57.3
14	7	370.4	0.8	341.8	2.5	364.6	0.6	7.3	105.4
14	4	364.7	1.0	342.4	2.5	360.5	1.1	7.5	95.5
14	1	357.1	1.2	343.8	2.5	354.9	1.4	7.4	94.8
8	10	373.0	1.0	344.5	1.8	367.6	-0.1	7.6	54.1
8	7	368.5	1.2	344.7	1.8	362.9	0.8	7.5	76.4
8	4	363.0	1.3	345.1	1.9	358.9	1.3	7.5	79.0
8	1	355.9	1.4	345.9	2.0	353.7	1.6	7.8	80.5
1	10	367.5	0.9	347.0	1.8	363.1	0.3	7.7	53.2
1	7	363.7	1.3	347.3	1.8	359.2	1.0	7.8	64.3
1	4	359.3	1.4	347.5	1.8	356.2	1.5	7.6	100.2
1	1	354.6	1.5	347.7	1.9	352.5	1.7	7.6	112.3

To summarize the results of the various simulations:

- The smaller the axial gap, the greater the deviation between the results for T_{max} and $T_{max,s}$, whereby it should be noted that the largest deviation is 1.5 % and 1.7 %, respectively.
- The smaller the radial gap, the greater the discrepancy between the results for T_{max} and $T_{max,s}$. For the T_{max}, the greatest deviation between a radial gap of 20 mm and one of 1 mm is 0.7 % and for $T_{max,s}$ 1.9 %. These largest deviations can be found at the largest axial gap.
- The deviation for $T_{max,g}$ is greater than for the other two temperatures, with the largest deviation of 3.7 %. A dependency of the deviation from the radial gap width cannot be determined. With regard to the axial gap width, the smaller it is, the smaller the deviation from $T_{max,g}$.
- Regarding the computing times, z88ENSI delivers results much faster. The speedup is between 6.9 and 15.0 and is even greater if not only a minimal model with pure heat conduction in the gap is simulated, but a real cask considering heat conduction, convection and thermal radiation. However, we would like to point out that the calculation times depend on many factors, including the available hardware. Therefore, the speedup will vary in other test settings.
- Overall, the results of z88ENSI are sufficiently accurate for the storage position by short computing times. Similar good results with a corresponding speedup are also achieved with the other positions (initial, handling, transport) and when considering convection and thermal radiation in the gaps.

4 CONCLUSION AND OUTLOOK

One of the fundamental requirements for dual purpose casks, which are used for the transport and interim storage of spent fuel assemblies, is the safe removal of the resulting decay heat. In order to ensure this and to determine the corresponding maximum temperatures at certain points, numerical simulations are

https://doi.org/10.1017/pds.2021.32 Published online by Cambridge University Press

used for the design and approval of DPCs. However, simulations can be very expensive for various reasons, especially when taking into account the insulating gas-filled gaps inside the cask.
Therefore, our goal is to develop a tool to receive fast and sufficiently accurate results for the three-dimensional thermal evaluation of DPCs. As we show, a three-dimensional approach is absolutely necessary in order to obtain more realistic results in comparison to the existing quasi-two-dimensional approach. We achieve the speedup compared to conventional simulations through the implementation of a new mesh manipulation tool and the extension of the thermal gap constrains. By manipulating the mesh four different positions (initial, storage, handling, transport) of the inner cask in the outer one and a wide variety of gap variations can be set. Concerning the thermal gap conditions, the basic idea is that the gaps between the inner an outer casks' inside are not meshed, but only their thermal behaviour is considered by using analytical equations. The newly implemented equations for the axial gaps and the already defined radial ones are added into the FEA systems of equations via nodal coupling. By doing this all heat transfer mechanisms and axial and radial heat flows could be considered case-specific.
In addition to the speedup, accuracy is essential. We can prove both through the validation presented in this paper. We compare the results of simulations with our tool, z88ENSI, with those generated with Ansys. The comparison is based on a minimal model and on three temperatures at critical positions for DPC. The largest deviations lie between -0.8% and 3.7% and the speedup is between 6.9 and 15.0.
In future work we will add other important thermal design and assessment criterions, such as the fuel rod cladding temperature. But there are also various boundary conditions that we will integrated to improve the accuracy of the results, for example the height-specific burn-up of the fuel assemblies or the heat transfer from the cask to the ground.

ACKNOWLEDGMENTS

This research projects were kindly supported by ENSI, Swiss Federal Nuclear Safety Inspectorate, Brugg, Switzerland.

REFERENCES

Cook, R., Malkus, D., Plesha, M., Witt, R. (2002), Concepts and Applications of Finite Element Analysis, John Wiley & Sons, Madison.
Dinkel, C., Billenstein, D., Roith, B., Rieg, F. (2019), 'Influence of gas-filled gaps on the thermal behaviour of dual purpose casks', in Proceedings of the 22nd International Conference on on Engineering Design (ICED 2019), Delft, The Netherlands, 05.08.2019 - 08.08.2019. https://dx.doi.org/10.1017/dsi.2019.159
Dinkel, C. (2019), *Integration analytischer Wärmeübertragungsberechnungsverfahren in das Finite-Elemente-System Z88 zur beschleunigten thermischen Bewertung von Transport- und Lagerbehältern für Brennelemente*, Dr-Ing., Universität Bayreuth.
Droste, B., Komann, S., Wille, F., Rolle, A., Probst, U., Schubert, S. (2014), 'Consideration of aging mechanism influence on transport safety of dual purpose casks for spent nuclear fuel or HLW', Packaging, Transport, Storage & Security of Radioactive Material, Vol. 25, pp. 105-112. https://doi.org/10.1179/1746510914y.0000000070
Fentiman, A., (2018), Radioactive Waste Management: Storage, Transport and Disposal. In: Nuclear Energy, 2nd ed. New York: Springer Nature, pp.241-250. https://doi.org/10.1007/978-1-4939-6618-9
Holtec International (n.d.), 'Safety Analysis Report on the HI-STAR 180 Package', Non-proprietary Version, Report HI-2073681, Revision 3, United States Nuclear Regulatory Commission, Marlton.
International Atomic Energy Agency IAEA (2018), 'Regulations for the Safe Transport of Radioactive Material: Specific Safety Requirements', No. SSR-6, Wien.
Marek, R., Nitsche, K. (2019), Praxis der Wärmeübertragung, Carl Hanser, München. https://doi.org/10.3139/9783446461253
Meetham, G. W., Van de Voorde, M. (2000), Materials for High Temperature Engineering Applications, Springer Vieweg, Berlin, Heidelberg. https://dx.doi.org/10.1007/978-3-642-56938-8
Petersen, C. (1983), *Literaturübersicht mechanischer und physikalischer Eigenschaften von Hüllrohrwerkstoffen für Fortgeschrittene Druckwasserreaktoren (FDWR) bei hohen Temperaturen*, Kernforschungszentrum Karlsruhe, Karlsruhe.
Reddy, J. N., Gartling, D.K. (2010), The Finite Element Method in Heat Transfer and Fluid Dynamics, CRC Press.
Rust, W. (2016), Nichtlineare Finite-Elemente-Berechnungen, Vieweg+Teubner Verlag, Wiesbaden. https://doi.org/10.1007/978-3-658-13378-8
Verein Deutscher Ingenieure VDI (2010), VDI Heat Atlas, Springer Vieweg, Berlin, Heidelberg.
Wriggers, P. (2006), Computational Contact Mechanics, Springer Berlin Heidelberg New York.